Vibrational−Rotational Spectra of HNS, NSH, and Their Ions: A Theoretical Study

Peter Gersdorf[†]

Institute of Organic Chemistry, University of Technology Dresden, D-01062, Dresden, Germany

Received: March 21, 1997; In Final Form: July 28, 1997[⊗]

The variational method is used to determine rotational−vibrational wave functions for HNS, NSH, and their ions from potential energy functions generated by high-level ab initio calculations. These wave functions describing the nuclear motion are then used in conjunction with ab initio dipole moment functions to predict radiative transition probabilities. Some spectroscopic constants are presented.

I. Introduction

Thionitrosyl hydride, HNS, is a relatively unknown molecule, although it corresponds to a classical structure in organic chemistry. Theoretical and experimental investigations about this molecule are useful for a better understanding of chemical reactions where HNS compounds might be short-lived intermediates. Moreover, such calculations are helpful for the search of this molecule in the interstellar space. HNS is considered as a model compound for thionitroso compounds RNS in organic chemistry, too.

Four years ago Ngyuen et al.[1] succeeded in detecting HNS or NSH by thermolysis of 1,3,4-oxathiazol-2-one in a collision−activation spectrum with a mass spectrometer. But this method does not allow detailed investigations of the structure and other properties. More than a decade ago thionitroso compounds RNS were identified as bridge ligands in iron complexes,[2] but their electronic structures as ligands in the complex are probably very different from the electronic structure of isolated HNS.

Some small molecules being isovalent with HNS are much better known. The FNS and the NSF systems have been studied quite intensively, both experimentally and by ab initio calculations.[3,4] The ground state of both isomers is a closed-shell singlet, the NSF isomer is obtained to be more stable than FNS. Also the HNO system has been discussed in great detail.[5,6] Transition-metal thionitrosyl complexes of the form M−NS have been studied several years ago.[7]

There are only a few ab initio calculations of HNS.[4,8−11] They indicate that HNS and NSH have closed-shell singlet electronic ground states with open-shell singlet and triplet excited states relatively low in energy. The HNS isomer is preferred to NSH by about 20 kcal mol^{-1}; the transition state connecting these two isomers lies 68 kcal mol^{-1} above HNS and 44 kcal mol^{-1} below the H + NS asymptote.[11] Both HNS and NSH are bent molecules with the bonding angles 108° and 110°, respectively. The NS bond length is shorter by 0.08 Å in NSH than in HNS;[10,11] this rectifies the counter-intuitive result of earlier workers.[4]

Collins and Duke[4] were the first authors to have calculated the equilibrium geometries of both isomers HNS and NSH in their lowest closed-shell states. They found (SCF, basis set is single-ζ cores, double-ζ valence S and P, 1d on S, extra p on N, and p on H) that HNS is more stable than NSH by 25.6 kcal mol^{-1} and that the NS bond length is shorter by 0.08 Å in HNS than in NSH. The latter fact was surprising in view of the conventional chemical picture (valence model) of a NS double bond in HNS and a triple bond in NSH from which the reverse order is expected. In fact this expectation has been confirmed by later more realistic and reliable work;[10,11] but simultaneously the naive idea of a triple NS bond in NSH became clear as too simple.[10,11] Mehlhorn et al.[8] found for HNS on the SCF-level (STO-3G) and with semiempirical methods (INDO, CNDO/S) that the energy of the first excited $n\pi^*$ singlet state S_1 is only 0.97 eV above the closed-shell ground-state S_0 (CNDO/S), whereas the corresponding $n\pi^*$ triplet state T_1 has been found even below S_0 (SCF/3-21G-level). With the adding of some correlation (MP2), this state sequence was reversed qualitatively:[8] the S_0 state was now lower than the T_1 state. Recently a new theoretical study of the molecular structure and spectra of HNS from Mehlhorn et al.[9] was published.

A very detailed study of the HNS system was made by Wasilewski and Staemmler.[10] They found that the lowest triplet, a $^3A''$ state, lies only 0.29 eV above the electronic ground state (X^1A'). The authors suppose that the reactivity of this triplet state is responsible for the difficulties of detecting HNS.[10] In analogy to HNO[6] the electronic ground state ($^1A'$) and the first excited singlet state ($^1A''$) of HNS correlate with a $^1\Delta$ state at linearity. The radiative transition probabilites between those two states are rather small; the vertical excitation energy amounts to about 1 eV.

Recently J. D. Watts and Ming-J. Huang[11] have performed high-level quantum chemical calculations (CCSD(T), MBPT-(2)) to obtain accurate structures, energies, and harmonic vibrational frequencies of the lowest singlet states of HNS and NSH (ground states).

This paper continues the above-mentioned theoretical (semiempirical and ab initio) studies of the H−N−S system by presenting high-level ab initio calculations for the so far unknown rotational vibrational spectra for the six system: HNS, HNS^+, HNS^-, NSH, NSH^+, and NSH^- ; for HNS part of its spectrum (between 1000 and 1600 cm^{-1}) is reported in ref 9. Some spectroscopic constants are given. The present work was undertaken in order to try to complete our knowledge of the rotational vibrational fundamentals of the H−N−S system; this should be of assistance in its experimental identification. As it is well-known, the infrared spectra of unstable molecules being absorbed in noble gas matrixes at low temperatures or existing in interstellar space are very powerful tools for their characterization.[12]

II. Computational Details

Within the Born−Oppenheimer approximation, the electronic Schrödinger equation is solved for a given geometry (being characterized by two bond lengths R_1 and R_2 and a bond angle θ).

[†] Permanent address: Dr. P. Gersdorf, Luchbergstrasse 6, D-01237 Dresden, Germany.

[⊗] Abstract published in *Advance ACS Abstracts,* October 15, 1997.

S1089-5639(97)01019-0 CCC: $14.00

TABLE 1: Calculated Geometry and Energy of $^1A'$ HNS[a]

	R(NS)	R(HN)	θ(HNS)	E
ref 10	3.01	1.95	107	−452.685 290
ref 11	3.001	1.936	108.28	−453.001 537
this work	3.011	1.958	107.8	−452.921 769

[a] Energy and bond lengths in au; bond angle in degrees.

TABLE 2: Calculated Geometry and Energy of $^1A'$ NSH[a]

	R(NS)	R(SH)	θ(NSH)	E
ref 10	2.88	2.66	109	−452.276 738
ref 11	2.860	2.648	109.71	−453.961 311
this work	2.857	2.616	110.86	−452.887 138

[a] Energy and bond lengths in au; bond angle in degrees.

In all calculations the Renner−Teller effect[13] and spin−orbit effects were not considered.

The Gaussian basis set used in the CASSCF calculations of the two lowest-energetic singlet and doublet states comprised 167 primitives contracted to 118 groups. For S, the 18s 13p basis of Partridge[14] was contracted and augmented by 3d functions (exponent: 1.9, 0.75, 0.23) and one f function (exponent: 0.5). In the 13s 8p basis of van Duijneveldt[15] for N, the innermost 7s and 3p functions were contracted and the basis set was augmented by 3d (exponent: 2.837, 0.968, 0.335) and one f (exponent: 1.093) functions of Dunning.[16] In the H basis set of van Duijneveldt,[15] the innermost 3s and 8s functions were contracted and the basis augmented with 3p functions (exponent: 1.8, 0.6, 0.2).

The active space in the (12, 9) CASSCF calculations for all 6 molecules consisted of the following 9 molecular orbitals: 6a′-12a′, 2a″-3a″. In the core regions, nine s functions were contracted at S, seven s functions and three p functions at N, and three s functions at H. In the special case of NSH CASSCF, wave functions were used for the MRCI(SD) calculations as reference functions, including all configurations with a weight larger than 0.01 in the configuration interaction expansions. Also the total energies, as well as energy differences (ionization energies and electron affinities) of the equilibrium geometries, cf. Tables 1−4, result from such MRCI(SD) calculations.

All the calculations of the electronic Schrödinger equations were performed with the MOLPRO'92 package.[17]

The energies and dipole moments have been calculated for 74 different geometries in the vicinity of the equilibrium geometries. The results were fitted to analytical expansions, see Appendix I. The program for the fit (also allowing for calculation of spectroscopic constants, see below) is due to J. Senekowitsch.[18] The energy function $E(R_1,R_2,\theta)$ is the potential energy of the Schrödinger equation for the nuclear motion, from which follow the vibrational and rotational eigenstates. The dipole moment function $\boldsymbol{\mu}(R_1,R_2,\theta)$ is needed additionally to calculate the (relative) intensities of transitions between them.

The Schrödinger equation for the nuclear motion (with the above-mentioned CASSCF or MRCI generated analytical input $E(R_1,R_2,\theta)$ has been solved variationally.[19] The Hamiltonian described by Handy[19] (use of the chain rule for partial differentiation) has six coordinates: the three internal coordinates and three Euler angles. Sums of products of harmonic oscillator eigenfunctions (in this work 15) and of the angular momentum and associated Legendre functions (in this work 32) served as trial wave functions. This procedure yields the positions of the absorption bands. The energy of the higher rotational vibrational levels were stable against a variation of the wave function within 2 cm^{-1}, of the lower levels within 0.1 cm^{-1}.

To also obtain the intensities of the absorption spectra, the integral absorption coefficients have been calculated with the standard equation;[21] here also the mentioned dipole moment functions $\mu_x(R_1,R_2,\theta)$ and $\mu_y(R_1,R_2,\theta)$ appear as input. Details of the calculations of vibrational rotational spectra are given in refs 22 and 23. The resulting intensities are plotted in Figures 1 and 2.

Finally the CASSCF (or MRCI) generated energy functions $E(R_1,R_2,\theta)$ are used to extract some spectroscopic constants such as rotation constants, harmonic frequencies, and anharmonic constants. This is done by quartic expansions of these energy functions around the equilibrium (near the equilibrium the energy function is truncated to quartic terms) and by standard second-order perturbation theory. Results are given in Table 5, Appendix II.

TABLE 3: Calculated Geometries, Ionization Energies, and Electron Affinities of HNS$^{\pm}$[a]

	R(NS)	R (HN)	θ (HNS)	ΔE
HNS^+	2.834 (2.76)	1.962 (1.93)	129.4 (130)	8.683 (8.88)
HNS^-	3.248 (3.25)	1.957 (1.97)	104.2 (103)	0.737 (1.03)

[a] R and θ as in Table 1, ΔE = IE (for the cation), and EA (for the anion) in EV. Results of ref 10 are in parentheses.

TABLE 4: Calculated Geometries, Ionization Energies, and Electron Affinities of NSH$^{\pm}$ [a]

	R(NS)	R(SH)	θ(NSH)	ΔE
NSH^+	2.931 (2.89)	2.631 (2.65)	100.3 (97)	9.181 (9.21)
NSH^-	3.043 (3.08)	2.709 (2.76)	111.8 (112)	0.427 (0.69

[a] R and θ as in Table 1, ΔE = IE (for the cation), and EA (for the anion) in EV. Results of ref 10 are in parentheses.

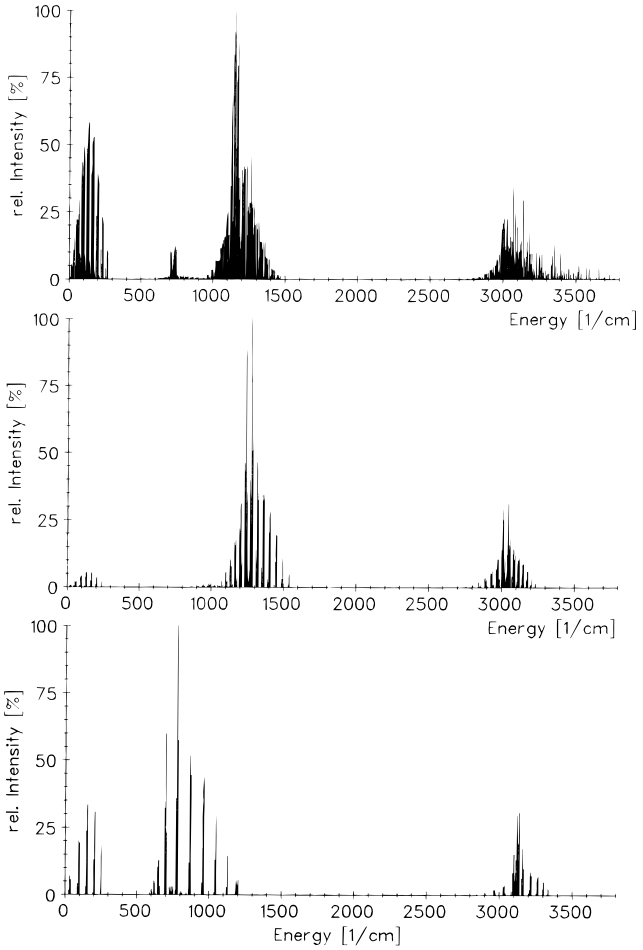

Figure 1. Theoretical absorption spectra of HNS^- (above $J \leq 12$), HNS (in the middle, $J \leq 7$), HNS^+ (below, $J \leq 5$) at 300 K with a resolution of 0.1*1 cm^{-1}. The transitions displayed correspond to the 000→ 000, 100, 010, and 001 bands.

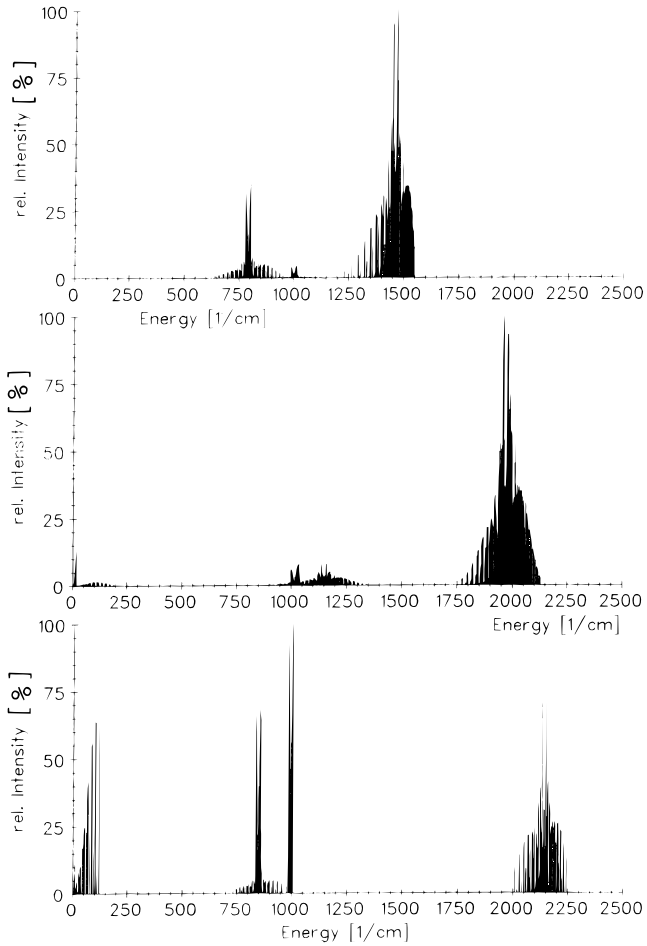

Figure 2. Theoretical absorption spectra of NSH^- (above, $J \leq 9$), NSH (in the middle, $J \leq 12$), NSH^+ (below, $J \leq 7$) at 300 K with a resolution of 0.1*1 cm^{-1}. The transitions displayed correspond to the 000→ 000, 100, 010, and 001 bands.

TABLE 5: Some Spectroscopic Constants[a]

	HNS^-	HNS [24]	HNS^+	NSH^-	NSH[b]	NSH^+
A	18.232	18.952	30.1305	10.3746	10.2581	9.3288
B	0.5452	0.622	0.6788	0.6399	0.7348	0.7026
C	0.5294	0.602	0.6639	0.6028	0.6857	0.6534
ω_1	736	980	775	790	1042	846
ω_2	1184	1280	1214	972	1163	1000
ω_3	3168	3220	3300	1847	2129	2217
x_{11}	−5.134	−6.563	−16.71	−9.2153	−14.352	−2.265
x_{22}	−13.29	−13.356	−7.88	11.332	−6.5274	−10.187
x_{33}	−80.88	−101.61	−90.64	−229.06	−71.195	−61.812
x_{12}	−10.40	−1.394	−0.6051	1.5659	−5.0782	5.674
x_{13}	0.3186	1.211	−3.603	28.41	9.3402	0.4124
x_{23}	−16.98	12.136	−0.8934	−12.69	3.3484	22.414
α_1^a	0.0433	0.033	−6.438	−0.01492	−0.1920	−0.202
α_2^a	−0.5751	−0.833	0.5549	−0.2109	−0.01159	−0.0343
α_3^a	0.7888	0.827	2.4497	0.7911	0.3966	0.3634
α_1^b	0.005	0.005	−0.0008	0.00657	−0.0004	−0.0018
α_2^b	0.0012	−0.001	0.0048	−0.00165	0.0058	0.006
α_3^b	−0.0001	0.0005	0.0013	−0.00956	−0.0017	−0.0054
α_1^c	0.005	0.005	0.0010	0.0081	0.005	0.0027
α_2^c	0.0027	0.0007	0.00477	−0.00006	0.0035	0.0053
α_3^c	0.0004	0.001	0.00234	−0.00628	−0.0002	−0.0031
G(000)	2420	2713	2503	1671	2053	1935

[a] In units of cm^{-1}. [b] MRCI level.

If not otherwise defined all results are given in atomic units (au), *R*(AB) means the bond length connecting A and B, and θ(ABC) is the bond angle.

III. Results and Discussion

The calculated molecular geometries and energies of HNS and NSH are shown in Tables 1 and 2 and compared with the results of the thorough theoretical studies of refs 10 and 11.

The shrinking of the NS bond length when going from HNS to NSH has been intensively discussed in terms of bond order[10,11] being two for HNS and greater than two but significantly less than three for NSH; the sulfur atom is hypervalent. Population analysis shows that the sulfur atom is 4 times more positively charged in NSH (N, −0.31; S, 0.19; H, 0.11) than in HNS (H, 0.22; N, −0.27; S, 0.05). The idea of a triple NS bond is an oversimplification; the bonding situation of NSH can be described rather by the limiting structures of a triple bond and ionic bond, i.e., it is a semipolar triple bond.[10]

The different charge distributions in HNS and NSH make also the dipole moment of NSH (1.03 au) remarkably larger than that of HNS (0.57 au). (Note that correlation lowers the dipole moment: for HNS the values calculated with CEPA,[10] CASSCF, and MRCI[9] are 0.61, 0.58, and 0.56 au, respectively).

The SH bond length in NSH is much larger than the NH bond length in HNS, in part because of the different sizes of S and N. This makes also the H atom more soft bound in NSH than in HNS; see the harmonic frequency ω_3 in Table 5.

The transition point connecting the two isomers is 2.88 eV above HNS and 1.94 eV above NSH. The state-of-art results of ref 11 are 2.95 and 1.91 eV, respectively.

The calculated molecular geometries of the ions $HNS^{\pm}$ and $NSH^{\pm}$ and their ionization energies (IE) or electron affinities (EA) are given in Tables 3 and 4 and compared with the results of ref 10.

How does the NS bond length change with ionization? Similarly to the cases HCS → HCS^- and HCO → HCO^- the bonds in the negative ion become larger and the equilibrium angle smaller than in the neutral species.[22] In the case of HNS the NS bond length decreases when going from HNS^- via HNS to HNS^+, because the detached electrons come mainly from a nonbonding (at the sulfur atom localized) molecular orbital; thus, the charge difference (effective charge of S minus effective charge of N) increases. In the case of NSH the NS length decreases again when going from NSH^- to NSH, but it increases for NSH to NSH^+, because the second detached electron comes mainly from a bonding (at S localized) molecular orbital. While in HNS the two electrons come from the same orbital, in NSH they come from different orbitals.

The electron affinities of $\lesssim$1 eV are in good agreement with other systems having unfilled antibonding molecular orbitals. The ionization energies are small and differ not so much from each other; this is because the highest occupied molecular orbital is nonbonding or even antibonding.

The ionization can be achieved theoretically in two steps: (i) vertical ionization (not changing the equilibrium geometry of the neutral molecule) and (ii) relaxation into the minimum of the ion. While for the cation the IE_{vert} is reduced by IE_{rel} (<0), the contribution due to relaxation, for the anion the EA_{vert} is enlarged by EA_{rel} (>0). That the anions are stable in the equilibrium geometry of the neutral molecule shows that electron correlation effects are sufficiently taken into account. As in other similar cases, EA_{rel} is also here only a small contribution (few percent) to EA. (Note that the corrections due to different zero-point energies, see last line of Table 5, are +0.04 eV for HNS^- and +0.05 eV for NSH^-.)

Altogether, Tables 1−4 show that the CASSCF (respectively MRCI) generated energies and dipole moments provide a

reliable basis to study vibrations, rotations and their corresponding absorption spectra of HNS, NSH, and their ions.

Figures 1 and 2 show the theoretical vibrational−rotational absorption spectra of HNS, NSH, and their ions which are here published for the first time (for HNS see refs 9 and 24). The resolution is 0.1 cm^{-1}; the assumed temperature is 300 K. The transitions displayed correspond to the 000 → 000 band (pure rotation) or to the 000 → 100, 010, 001 vibrational bands. The spectrum of NSH is based on fits of MRCI calculations, whereas all the other spectra are based on CASSCF results. Further details of these calculations are available on request.

The calculations were made for differently chosen rotation quantum numbers J, from $J_{min} = 0$ to J_{max}. Here J_{max} is different for different systems (cf. Figures 1 and 2). As known, the change of the values of J_{max} are not very important: if J_{max} of one spectrum is increased, then this spectrum would not change significantly; it would become more dense and the width of each band would increase only somewhat.

It can be seen in the Figures 1 and 2 that different molecules are characterized by different positions and intensities of the bands. In the case of HNS^+ the distances of the lines within one band are somewhat larger than those of the other molecules. This is connected in this case with the larger rotation constant A (cf. Table 5) and in the end with the large value of θ (HNS). The pure rotation band of NSH^- has very low intensities; note that to a good approximation purely rotational transitions depend, for a neutral species, on the magnitude of the permanent electric dipole moment in the vibrational ground state and, for an ion, on the distance between center of charge and center of mass.[22] The highest energy bands arise mostly from the H−N or the S−H stretching vibration, respectively, whereas the other two vibration bands arise mostly from the N−S vibration and the angle deformation. Due to the small electron affinity of NSH (= ionization energy of NSH^- = 0.42 eV), all vibrational rotational states of NSH^- lying above this energy (3388 cm^{-1}) will undergo a rapid detachment of an electron. (For HNS^- these figures are 0.74 eV = 5969 cm^{-1}.) The ω_2 band of HNS (see Figure 1, middle, 1000−1600 cm^{-1}) agrees with Figure 4 of Mehlhorn et al.[9]

Some spectroscopic constants (rotation constants, harmonic frequencies, anharmonic constants, zero-point energies (ZPE), and α-constants representing the interaction of the rotation and vibration) are presented in Appendix II, Table 5.

The harmonic frequencies of HNS and NSH presented here agree quite well with those of ref 11: HNS (1015, 1233, and 3379 cm^{-1}) and NSH (1034, 1147, and 2189 cm^{-1}).

The harmonic frequencies ω_3 describe the H−N respectively S−H stretch (while the other modes are mixtures of the N═S, respectively, N^-═S^+ stretch and the bend). That they are so much larger in the HNS system than in the NSH system may be understood in terms of the different bond lengths R (HN) and R (SH), see Tables 1-4; the more distant H atom is softer bound.

The harmonic frequencies ω_1, ω_2, and ω_3 are closer to each other in NSH than those in HNS. So more coordinate or mode mixing is to be expected, which may be the reason for ω_2 being smaller in NSH than in HSN despite NS being stronger bound in NSH than in HSN. In NSH^- the ω's are even closer to each other. This is similar to HCS (3208.7, 1178.2, and 875.9 cm^{-1}) and HCS^- (2819.1, 1162.3, and 922.8 cm^{-1}), where the CS stretching vibration has the middle harmonic frequency of HCS, while in HCS^- it has the lowest frequency (the order with the angle bending mode is reversed).[22]

Note that $^1/_2(\omega_1 + \omega_2 + \omega_3)$ the harmonic estimate of the ZPE, is greater than G(000) due to anharmonicity. Furthermore, the molecule becomes softer (as measured by the ZPE) when going from the neutral molecule via the cation to the anion.

Acknowledgment. I thank A. Mehlhorn (Dresden) for suggesting the subject, P. Rosmus and W. Gabriel (Frankfurt a. M.) for programs enabling me to calculate the spectra, R.D. Gordon and G. Smith (Kingston) for critically reading the manuscript, and the Deutsche Forschungsgemeinschaft supporting this work.

Appendix I

Analytical Expansions of the Energy and Dipole Moment. For the analytical expansion of the electronic ground-state energy $E(R_1,R_2,\theta)$ the Simons−Parr−Finlan bond stretching coordinates (depending on $R_{1,2}$)[25] and the Carter−Handy angle-bending coordinate (a cubic polynomial of the displacement coordinate $\theta-\theta^E$)[22,23] were chosen,

$$E(R_1,R_2,\theta) = \sum_{i=0}^{5}\sum_{j=0}^{5}\sum_{k=0}^{5} C_{ijk}^{E}\left(1-\frac{R_1^E}{R_1}\right)^i\left(1-\frac{R_2^E}{R_2}\right)^j \times [A_0(\theta-\theta^E) + A_1(\theta-\theta^E)^2 + A_2(\theta-\theta^E)^3]^k$$

with $A_0 = 1.5$, $A_1 = [3 - 2A_0(\pi - \theta^E)]/(\pi - \theta^E)^2$, $A_2 = -^1/_3[A_0 + 2A_1(\pi - \theta^E)]/(\pi - \theta^E)^2$. This latter construction means that, for $\theta = \pi$, the θ-polynomial takes the value 1 and its derivative vanishes.

For the analytical expansion of the 2 components of the dipole moment $\boldsymbol{\mu}(R_1,R_2,\theta)$ displacement coordinates were chosen:

$$\mu_{x,y}(R_1,R_2,\theta) = \sum_{i=0}^{5}\sum_{j=0}^{5}\sum_{k=0}^{5} C_{ijk}^{\mu_{x,y}}(R_1 - R_1^{\mu})^i(R_2 - R_2^{\mu})^j(\theta - \theta^{\mu})^k$$

For a given geometry (R_1,R_2,θ) the solution of the electronic Schrödinger equation yield *SE* and $\mu_{x,y}$, the left-hand sides of the above equations. With the results for several geometries the expansion coefficients C_{ijk}^{E}, $C_{ijk}^{\mu_x}$, $C_{ijk}^{\mu_y}$, are determined by a minimizing procedure.[18] Further details are available on request.

Appendix II

Some Spectroscopic Constants. Some spectroscopic constants calculated by means of second-order perturbation theory are given in Table 5. After the fits of the ground-state energy surfaces and the corresponding dipole moment surfaces, a Wilson FG analysis was carried out. The Watson Hamiltonian[26] with its three normal coordinates and three Euler angles can be divided into a zeroth-order term (rigid rotator and harmonic oscillator) and a small remainder.

References and Notes

(1) Nguyen, M. T.; van Quickenborne, L. G.; Plisner, M.; Flammang, R. *Mol. Phys.* **1993**, *78*, 111. The same authors have studied the related system H_2NS and its ionic counterparts in *J. Chem. Phys.* **1994**, *101*, 4885.

(2) Herberhold, M.; Bühlmeyer, W. *Angew. Chem.* **1984**, *96*, 64.

(3) So, S. P.; Richards, W. G. J. *J. Chem. Soc., Faraday Trans.* 2 **1978**, *74*, 1743. Seeger, R.; Seeger, U.; Bartetzko, R.; Gleiter, R. *Inorg. Chem.* **1982**, *21*, 1743. Zirz, C.; Ahlrichs, R. *Inorg. Chem.* **1984**, *23*, 26. Schaad, J. L. J.; Hess, B. A.; Cársky, P.; Zahradnik, R. *Inorg. Chem.* **1984**, *23*, 2428. Cook, R. L.; Kirchhoff, W. H. *J. Chem. Phys.* **1967**, *47*, 4521.

(4) Collins, M. P. S.; Duke, B. J. *J. Chem. Soc., Dalton Trans.* **1978**, 277.

(5) Nomura, O. *Int. J. Quantum Chem.* **1980**, *18*, 143. Heibers, A.; Almlöf, J. *J. Chem. Phys. Lett.* **1982**, *85*, 542. Johns, J. W. C.; McKellar, A. R. W.; Weinberger, E. *Can. J. Phys.* **1983**, *61*, 1106.

(6) Bruna, P. J. *Chem. Phys.* **1980**, *49*, 39.

(7) Herberhold, M. *Nachr. Chem., Tech. Lab.* **1981**, *29*, 365. Roesky, H. W.; Pandey, K. K. *Adv. Inorg. Chem. Radiochem.* **1983**, *26*, 337.

(8) Mehlhorn, A.; Sauer, J.; Fabian; J., Mayer, R. *Phosphorus Sulfur* **1981**, *11*, 325.

(9) Mehlhorn, A.; Fabian, J.; Gabriel, W.; Rosmus, P. *J. Mol. Struct. (THEOCHEM)* **1995**, *339*, 219.

(10) Wasilewski, J.; Staemmler, V. *Inorg. Chem.* **1986**, *25*, 4221.

(11) Watts, J. D.; Huang, M.-J. *J. Phys. Chem.* **1995**, *99*, 5331.

(12) Hess, B. A.; Schaad, L. J.; Cársky, P.; Zahradnik, R. *Chem. Rev.* **1986**, *86*, 709.

(13) Renner, R. *Z. Phys.* **1934**, *92*, 172. Petelin, A. N.; Kiselev, A. A. *Int. J. Quantum Chem. VI* **1972**, 711. Jungen, Ch.; Merer, A. J. *Mol. Phys.* **1980**, *40*, 1. Jungen, Ch.; Merer, A. J. *Mol. Phys.* **1980**, *40*, 95. Petrolongo, C. *J. Chem. Phys.* **1988**, *89*, 1297. Aguilar, A.; Gonzalez, M.; Poluyanov, L. V. *Mol. Phys.* **1992**, *72*, 193.

(14) Partridge, H. R. NASA Technical Memorandum. NASA, Washington, DC, 1987; 89449.

(15) van Duijneveldt, F. B. IBM Research Report. IBM Corp. 1971, R. J.945.

(16) Dunning, T. H. *J. Chem. Phys.* **1989**, *90*, 1007.

(17) The ab initio program package MOLPRO was written by Werner, H. J., and Knowles, P. J., with contributions of Almlöf, J.; Elbert, S.; Meyer, W.; Reinsch, E.-A.; Pitzer, R.; Stone, A.

(18) Senekowitsch, J., PhD Thesis, Universität Frankfurt a. M., 1988.

(19) The programs for such calculations are due to S. Carter.

(20) Handy, N. C. *Mol. Phys.* **1987**, *61*, 207.

(21) Smith, M. H. A.; Rinsland, C. P.; Fridovich, B.; Rao, K. N. *Molecular Spectroscopy: Modern Research*; Academic Press: London, 1985; Vol. 3, pp 111.

(22) Carter, S.; Senekowitsch, J.; Handy, N. C.; Rosmus, P. *Mol. Phys.* **1988**, *65*, 143. Senekowitsch, J.; Carter, S.; Werner, H.-J.; Rosmus, P. *J. Chem. Phys.* **1988**, *88*, 2641. Senekowitsch, J.; Carter, S.; Rosmus, P.; Werner, H.-J. *Chem. Phys.* **1990**, *147*, 281.

(23) Carter, S.; Handy, N. C. *Mol. Phys.* **1982**, *47*, 1445. Carter, S.; Handy, N. C.; Sutcliffe, B. T. *Mol. Phys.* **1983**, *49*, 745. Carter, S.; Handy, N. C. *Mol. Phys.* **1984**, *52*, 1367. Carter, S.; Handy, N. C. *Mol. Phys.* **1984**, *53*, 1033. Carter, S.; Handy, N. C. *J. Chem. Phys.* **1987**, *81*, 4294. Carter, S.; Handy, N. C.; Rosmus, P.; Chambaud, G. *Mol. Phys.* **1990**, *71*, 605.

(24) Gabriel, W. PhD Thesis, Universität Frankfurt a. M., 1994.

(25) Somins, G.; Parr, R. G.; Finlan, J. M. *J. Chem. Phys.* **1973**, *59*, 3229.

(26) Watson, J. K. G. *Mol. Phys.* **1970**, *19*, 465.